RESEARCH ARTICLE

Burkholderia pseudomallei Penetrates the Brain via Destruction of the Olfactory and Trigeminal Nerves: Implications for the Pathogenesis of Neurological Melioidosis

James A. St. John,[a] Jenny A. K. Ekberg,[a,b] Samantha J. Dando,[c] Adrian C. B. Meedeniya,[a] Rachel E. Horton,[c] Michael Batzloff,[c] Suzzanne J. Owen,[c] Stephanie Holt,[c] Ian R. Peak,[c,d] Glen C. Ulett,[c,d] Alan Mackay-Sim,[a] Ifor R. Beacham[c]

Eskitis Institute for Drug Discovery, Griffith University, Brisbane, Queensland, Australia[a]; School of Biomedical Sciences, Queensland University of Technology, Brisbane, Queensland, Australia[b]; Institute for Glycomics, Griffith University, Gold Coast, Queensland, Australia[c]; School of Medical Science, Griffith University, Gold Coast, Queensland, Australia[d]

J.A.S.J. and J.A.K.E. contributed equally to this article.

ABSTRACT **Melioidosis is a potentially fatal disease that is endemic to tropical northern Australia and Southeast Asia, with a mortality rate of 14 to 50%. The bacterium *Burkholderia pseudomallei* is the causative agent which infects numerous parts of the human body, including the brain, which results in the neurological manifestation of melioidosis. The olfactory nerve constitutes a direct conduit from the nasal cavity into the brain, and we have previously reported that *B. pseudomallei* can colonize this nerve in mice. We have now investigated in detail the mechanism by which the bacteria penetrate the olfactory and trigeminal nerves within the nasal cavity and infect the brain. We found that the olfactory epithelium responded to intranasal *B. pseudomallei* infection by widespread crenellation followed by disintegration of the neuronal layer to expose the underlying basal layer, which the bacteria then colonized. With the loss of the neuronal cell bodies, olfactory axons also degenerated, and the bacteria then migrated through the now-open conduit of the olfactory nerves. Using immunohistochemistry, we demonstrated that *B. pseudomallei* migrated through the cribriform plate via the olfactory nerves to enter the outer layer of the olfactory bulb in the brain within 24 h. We also found that the bacteria colonized the thin respiratory epithelium in the nasal cavity and then rapidly migrated along the underlying trigeminal nerve to penetrate the cranial cavity. These results demonstrate that *B. pseudomallei* invasion of the nerves of the nasal cavity leads to direct infection of the brain and bypasses the blood-brain barrier.**

IMPORTANCE **Melioidosis is a potentially fatal tropical disease that is endemic to northern Australia and Southeast Asia. It is caused by the bacterium *Burkholderia pseudomallei*, which can infect many organs of the body, including the brain, and results in neurological symptoms. The pathway by which the bacteria can penetrate the brain is unknown, and we have investigated the ability of the bacteria to migrate along nerves that innervate the nasal cavity and enter the frontal region of the brain by using a mouse model of infection. By generating a mutant strain of *B. pseudomallei* which is unable to survive in the blood, we show that the bacteria rapidly penetrate the cranial cavity using the olfactory (smell) nerve and the trigeminal (sensory) nerve that line the nasal cavity.**

Received 9 January 2014 **Accepted** 14 March 2014 **Published** 15 April 2014

Citation St. John JA, Ekberg JAK, Dando SJ, Meedeniya ACB, Horton RE, Batzloff M, Owen SJ, Holt S, Peak IR, Ulett GC, Mackay-Sim A, Beacham IR. 2014. *Burkholderia pseudomallei* penetrates the brain via destruction of the olfactory and trigeminal nerves: implications for the pathogenesis of neurological melioidosis. mBio 5(2):e00025-14. doi:10.1128/mBio.00025-14

Invited Editor Paul Brett, University of South Alabama **Editor** Patricia Johnson, UCLA

Address correspondence to Ifor R. Beacham, beacham@griffith.edu.au.

Melioidosis is a potentially fatal disease endemic to the tropics, particularly northeastern Thailand and northern Australia, where the mortality rates approach 50% and 14%, respectively (1). Melioidosis is also considered to be underreported and an emerging disease worldwide (1). Clinical presentations of melioidosis vary, ranging from chronic to acute disease and potentially rapid death due to systemic infection and septic shock (1–3). Virtually any organ of the body may be infected; while skin and soft tissues, including lungs, liver, and spleen, are often involved, the bacteria that cause melioidosis can also infect the parotid gland, the brain, and bone (1, 3).

Burkholderia pseudomallei, the causative agent of melioidosis, is easily isolated from soil and standing water in regions of endemicity. Infection of humans stems from environmental exposure and is closely associated with high rainfall (4). Two common routes of inoculation are thought to be percutaneous inoculation and inhalation; inhalation of contaminated water droplets or dust (soil) is probably the most important natural route of infection. Animal studies of melioidosis using inhalational exposure and intranasal inoculation demonstrate infection of the lung and systemic infection of internal organs. Such studies have revealed previously unrecognized sites of colonization in the nasal mucosa-associated lymphoid tissue (NALT) and in the nasal mucosa, especially the olfactory epithelium (5). This suggests that respira-

tory infection and nasal colonization may be a portal of entry to the brain and blood without necessarily involving the lower respiratory tract (5).

Neurological abnormalities in human melioidosis (neurological melioidosis) are various, and direct invasion of the central nervous system (brain stem, cerebellum, and spinal cord) occurs in at least some cases (6, 7). Clinically, nearly all such cases (5% of total cases) in the Royal Darwin Hospital prospective study featured brain stem involvement (brain stem encephalitis) (6, 7), although cases in Singapore appear to present more frequently as micro- and macroabscess patterns and may represent systemic spread via the blood (8).

It has been suggested previously (6) that classical neurological melioidosis, with involvement of brain stem, cerebellum, and spinal cord, is due to direct central nervous system invasion, but the route of infection is unknown. It also has been suggested (6) that *B. pseudomallei* may travel along nerves, and recent evidence in an animal model provides compelling evidence for direct infection of the brain via the nose in the absence of bacteremia (5).

The nasal mucosa comprises the respiratory epithelium, located in the inferior-anterior nasal cavity, and the olfactory epithelium, located in the superior-posterior nasal cavity. The olfactory epithelium contains the olfactory receptor neurons, whose axons extend all the way from the nasal cavity to the olfactory bulb in the brain (Fig. 1A to D). The olfactory nerve fascicles that lie within the lamina propria underneath the epithelium coalesce to form larger nerve bundles that project through the bony cribriform plate to enter the central nervous system where they form the nerve fiber layer of the olfactory bulb (Fig. 1B and D). Thus, the olfactory nerve constitutes a direct conduit from the nasal cavity to the brain. The nasal mucosa is also innervated by the ophthalmic branch of the trigeminal nerve, a sensory nerve providing tactile, pain, and temperature sensitivity to the nose. Thus, the trigeminal nerve could also provide a direct route from nasal mucosa to the brain and be of particular importance to neurological melioidosis with brain stem encephalitis (1, 7).

Infection of the brain via the olfactory nerve has been demonstrated for many viruses (9–15) and also in the case of certain amoebae which infect the olfactory bulb, causing a necrotizing meningoencephalitis (11, 16, 17), but it is rarely described for bacteria. There is some evidence that *Listeria monocytogenes* enters trigeminal nerve axon terminals and is retrogradely transported to the brain stem, resulting in brain stem encephalitis (18). There are also reports that, following intranasal infection of mice, *Streptococcus pneumoniae* may enter the brain via the olfactory nerve (19) and that *Neisseria meningitidis* can infect the meninges by this route (20).

We have previously demonstrated that *B. pseudomallei* rapidly infects the olfactory epithelium and the olfactory bulb (5). Our findings further suggested that the olfactory nerve in the olfactory mucosa is a conduit for *B. pseudomallei* infection of the brain. The aims of the current study were (i) to describe expanded evidence for brain invasion by *B. pseudomallei* through the olfactory nerve, (ii) to gain further insight into the mechanisms by which the bacteria invade nasal tissue and travel along the olfactory nerve, and (iii) to determine if the trigeminal nerve, which also innervates the olfactory epithelium, is also involved in brain infection.

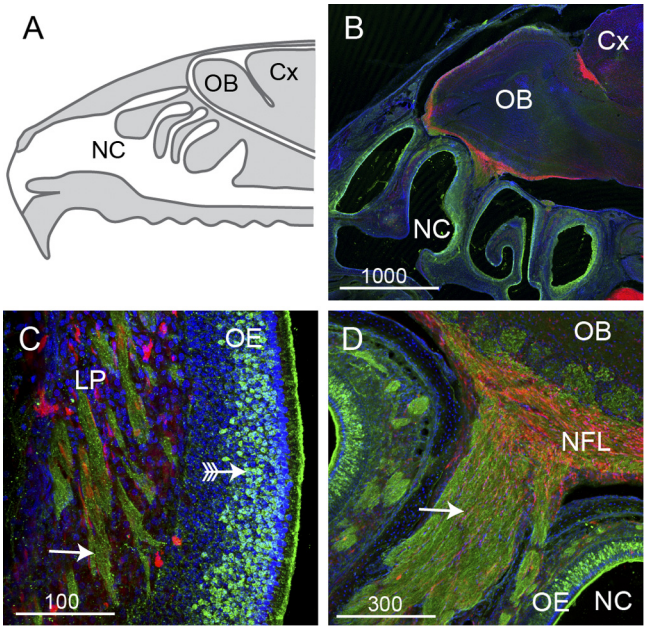

FIG 1 The olfactory system is a potential portal of entry into the brain. (A) Schematic sagittal view of the nasal cavity (NC), olfactory bulb (OB), and cerebral cortex (Cx). (B to D) Panels show sagittal sections from S100β-DsRed transgenic mice immunolabeled with antibodies against olfactory marker protein (OMP; green); olfactory ensheathing cells and chondrocytes express DsRed, and nuclei are stained with DAPI (blue). (B) Low-power view of the nasal cavity and olfactory bulb; this image is a montage of four fields of view that have been spliced together. (C) Within the olfactory mucosa, neurons (green; arrow with tail) reside in the olfactory epithelium (OE) and project their axons in bundles (arrows) through the lamina propria (LP). Olfactory ensheathing cells (red) surround the axon bundles. (D) The axon bundles merge together to form a large nerve (arrow) that passes into the nerve fiber layer (NFL) which lines the outer layer of the olfactory bulb. Bar sizes are in μm.

RESULTS

***Burkholderia pseudomallei* destroys and penetrates the olfactory epithelium.** To determine how *B. pseudomallei* colonizes the olfactory nerve, we intranasally inoculated adult mice with an isogenic acapsular mutant strain of *B. pseudomallei* (MSHR520Δ*cap*) for 24 to 48 h and then examined cryostat sections of the infected nasal cavity. The capsule prevents phagocytosis and is essential for bacterial survival in blood; thus, the Δ*cap* mutant strain is unable to survive in the bloodstream. As hematogenous brain infection is eliminated, brain infection via nerves extending from the nasal cavity into the brain can be studied in isolation. After 24 to 48 h of exposure, bacteria were detected by immunohistochemistry within the nasal cavity (Fig. 2A). While bacteria were detected in both the left and the right sides of the nasal cavity, there was often one side in which bacteria were more numerous (arrow, Fig. 2A). The healthy olfactory epithelium is a thick uniform stratified layer in the dorsal region of the nasal cavity (Fig. 2B), while the respiratory epithelium is a thin layer that lines the ventral and rostral nasal cavity (Fig. 2B). After exposure to intranasally delivered *B. pseudomallei*, the olfactory epithelium dramatically altered morphology and was crenellated with large swellings adjacent to where the bacteria were present in high numbers (arrow with tail, Fig. 2C). In comparison, the respiratory epithelium showed no gross morphological changes (Fig. 2C).

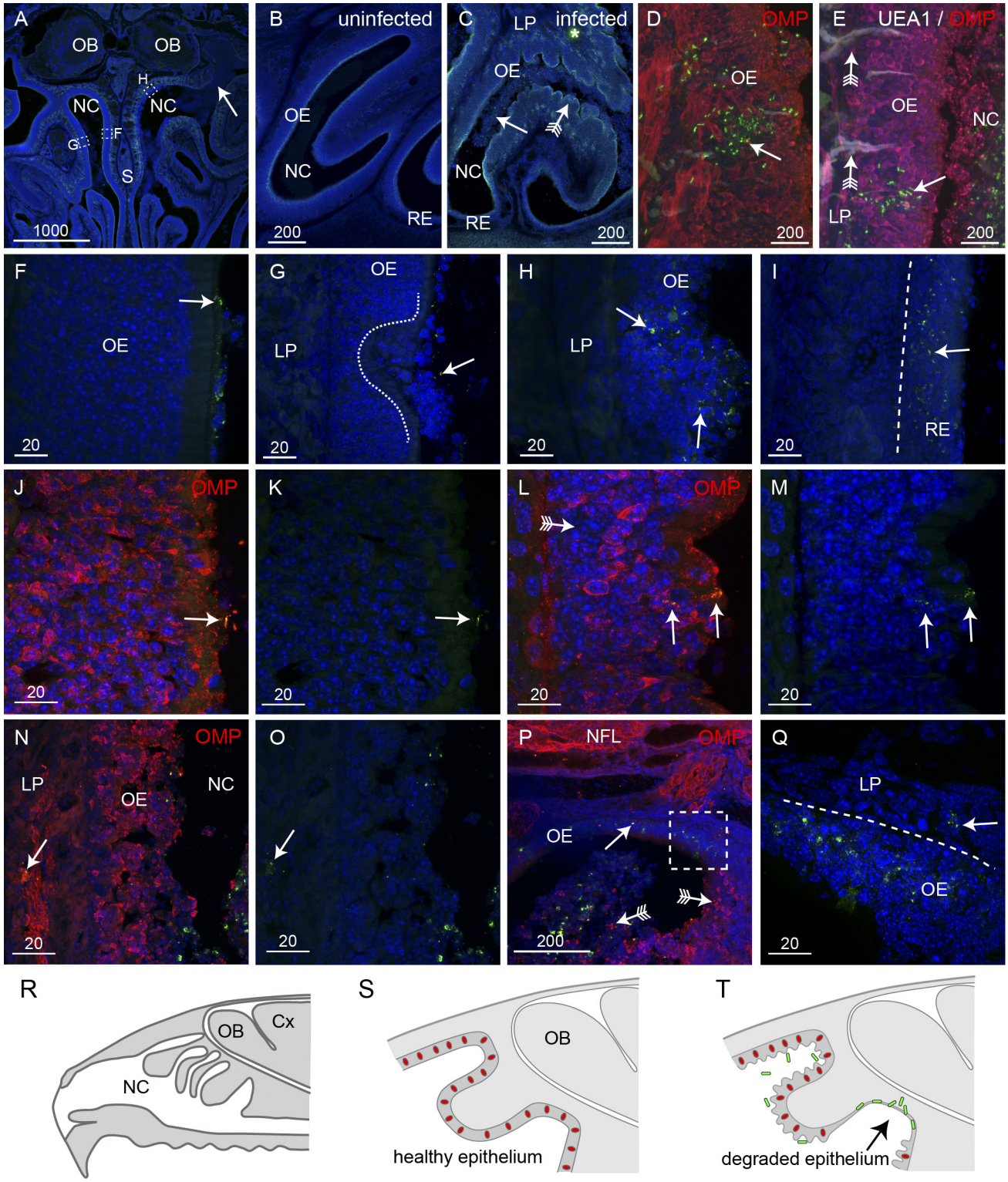

FIG 2 *B. pseudomallei* penetrates degraded olfactory and intact respiratory epithelium (RE). All sections were immunolabeled with anti-*B. pseudomallei* antibodies (green) and DAPI (blue); some were also labeled with anti-OMP antibodies and UEA1 lectin as indicated. (A) A coronal section of the nasal cavity (NC) shows that one side has extensive infection (arrow) while the other side has little evidence of infection. Boxed areas are shown in panels F to H as indicated. (B) A higher-magnification view of uninfected olfactory epithelium (OE) shows a uniform structure. (C) OE in an inoculated mouse shows an extensive presence of *B. pseudomallei* (arrow; green) in the NC at 24 h. The OE is crenellated (arrow with tail); the thin respiratory epithelium (RE) in the ventral NC was not visually affected. The asterisk indicates nonspecific autofluorescence. (D) Bacteria (green) occasionally penetrated relatively intact epithelium, but only in patches where neurons (immunolabeled with OMP; red) were absent (arrow). (E) In the olfactory epithelium, bacteria (green; arrow) were not associated with Bowman's glands (labeled with UEA1 lectin; white; arrow with tail); olfactory neurons (red) are labeled with anti-OMP antibodies. (F to H) Higher-magnification views of

(Continued)

We next examined the olfactory epithelium at higher magnification to determine where the bacteria penetrated it. On a few rare occasions, we detected *B. pseudomallei* within relatively intact epithelium, but only in regions where neurons were absent (Fig. 2D). In these regions, we considered that bacteria could have penetrated Bowman's glands, which are the mucous secretory ducts that lie within the epithelium. However, lectin staining with UEA1, which we find is a marker of Bowman's glands, showed that the bacteria were not present in the glands (arrows with tail, Fig. 2E). We then compared the regions of olfactory epithelium in which bacteria were in close proximity. In regions where small numbers of bacteria were present in the mucous layer that lines the apical surface of the epithelium, the olfactory epithelium showed no gross morphological changes (arrow, Fig. 2F). In areas where the epithelium showed signs of ulceration and indentation, bacteria were again present immediately adjacent to but not within the olfactory epithelium (Fig. 2G). It was only when the structural integrity of the epithelium was obviously degraded that bacteria were able to penetrate the olfactory epithelium (Fig. 2H). In contrast, in the respiratory epithelium, bacteria easily penetrated the epithelium without any gross morphological changes to the structural integrity of the epithelium (Fig. 2I). We confirmed that the structural integrity of the olfactory epithelium had degraded by immunolabeling with antibodies against olfactory marker protein (OMP), which is expressed by all primary olfactory neurons and their axons. When bacteria were present in the mucosal layer on the apical surface of the epithelium (arrow, Fig. 2J and K), OMP immunolabeling was uniform throughout the olfactory epithelium (Fig. 2J). In contrast, in areas with partial penetration of *B. pseudomallei* into the epithelium, the neuronal layer showed clear signs of disruption and the OMP immunolabeling was not uniform, with some areas showing low levels of OMP immunoreactivity (Fig. 2L). In regions where the epithelium showed extensive degradation, OMP immunolabeling revealed that the cells had lost their normal structural morphology (compare Fig. 2N with 2J). Even in these regions of epithelium, however, only a small number of bacteria were detected within the epithelial layer. Some bacteria had penetrated the epithelium, reaching the olfactory nerve bundles within the lamina propria (arrow, Fig. 2N and O). On the few occasions when *B. pseudomallei* was present in the epithelium in which olfactory neurons were intact, the bacteria were not localized near intact neurons but instead were in small pockets of degraded epithelium (arrow, Fig. 2D and E). It was only when the neuronal layer of the epithelium had been lost and shed off into the nasal cavity (arrows with tails, Fig. 2P) that the bacteria penetrated the remaining layer of the olfactory epithelium and underlying lamina propria (Fig. 2P and Q). In summary, in healthy uninfected mice, the olfactory epithelium that lines the rostral-dorsal regions of the nasal cavity is uniform and the olfactory sensory neurons are distributed throughout the layer (Fig. 2R and S). Infection by *B. pseudomallei* results in widespread crenellation of the olfactory epithelium, but the neuronal layer generally remains intact and bacteria cannot penetrate the epithelium. It is only when neurons are lost from the epithelium that bacteria can penetrate the underlying layers (Fig. 2T).

***Burkholderia pseudomallei* migrates along olfactory nerve fascicles that are devoid of axons.** The neurons that reside in the olfactory epithelium project their axons to the olfactory bulb in bundles of axons called fascicles (Fig. 1C). As it was clear that *B. pseudomallei* penetrated the olfactory epithelium only when the neuronal layer had been perturbed, we next examined the morphology of the axon fascicles in which *B. pseudomallei* was present. Despite the extensive crenellation of the olfactory epithelium and the presence of bacteria within the nasal cavity (Fig. 3A), the bacteria were detected within only a small number of olfactory axon fascicles within the lamina propria (Fig. 3C to E). It should be noted that due to the angle of the cryostat sectioning, the axons in fascicles lying within the lamina propria do not necessarily arise from neurons in the adjacent epithelium but are likely to arise from neurons some distance away. Hence, the infected axon fascicles sometimes lay adjacent to regions of relatively intact epithelium in which no bacteria were detected (Fig. 3C and E).

In all axon fascicles in which *B. pseudomallei* was detected, the bacteria were present in areas in which OMP immunoreactivity was absent, indicating that the axons had degenerated and that thus only the hollow conduit consisting of glial cells and a few axons remained (Fig. 3B, C, E, and F). OMP immunolabeling was restricted to the periphery of the axon fascicles, indicating that the few surviving axons were localized to the periphery (arrows with tails, Fig. 3E). In contrast, in axon fascicles in which bacteria were not detected and which were adjacent to epithelium that showed loss of morphological integrity, the axon fascicles showed uniform OMP immunoreactivity (arrow with tail, Fig. 3G and H). In axon fascicles in which bacteria were present, we examined the structure of the glia, called the olfactory ensheathing cells (OECs), that normally surround the axons. The olfactory ensheathing cells appeared intact and showed no gross morphological changes (Fig. 3D; see also Movie S1 in the supplemental material), indicating that it is only the axons that are destroyed by the presence of the bacteria. Closer to the olfactory bulb, the axon fascicles coalesce to form a large nerve bundle (arrow, Fig. 3I). In this region, too, axons were absent from areas in which *B. pseudomallei* was

Figure Legend Continued

the boxed areas indicated in panel A. (F) *B. pseudomallei* (arrow) was present on the surface of the OE, but no morphological reaction was apparent. (G) Ulceration of the OE (dashed line) was seen, although the presence of bacteria was limited (arrow). (H) The OE showed extensive destruction and loss of integrity, and bacteria were present (arrows) within the epithelium. Bacteria were not detected in the lamina propria (LP) underlying the OE (G and H). (I) In patches of respiratory epithelium, there was widespread infection with *B. pseudomallei* (arrow), but bacteria did not penetrate the deeper layers. (J and K) OMP immunolabeling (red) demonstrates that healthy epithelium was not penetrated by bacteria (arrow) despite their presence in the adjacent nasal cavity, but that epithelium was penetrated as the neurons partially degraded; panel K shows the same section as that in panel J but with the red channel (OMP) turned off. (L to O) OMP immunolabeling became patchy with some areas showing low levels of OMP reactivity (arrow with tail). Bacteria penetrated the outer layers and were present in nerve bundles in the lamina propria (arrows in panels N and O); panels M and O show the same sections as those in panels L and N, respectively, but with the red channel (OMP) turned off. (P and Q) Complete loss of the neuronal layer led to colonization of the remaining layer by bacteria (arrows); arrows with tails point to neurons in the nasal cavity and remaining epithelium. (R to T) Schematics summarizing the infection of the epithelium. (R) Sagittal view of the nasal cavity, olfactory bulbs (OB), and cortex (Cx). (S) In uninfected mice, the olfactory epithelium is uniform and neurons (red) are distributed throughout the epithelium. (T) When *B. pseudomallei* (green) is present, the majority of epithelium becomes crenellated but neurons remain within the epithelium and bacteria cannot penetrate. In some regions, the neurons are lost (arrow) and bacteria penetrate the remaining layers. Bar sizes are in μm.

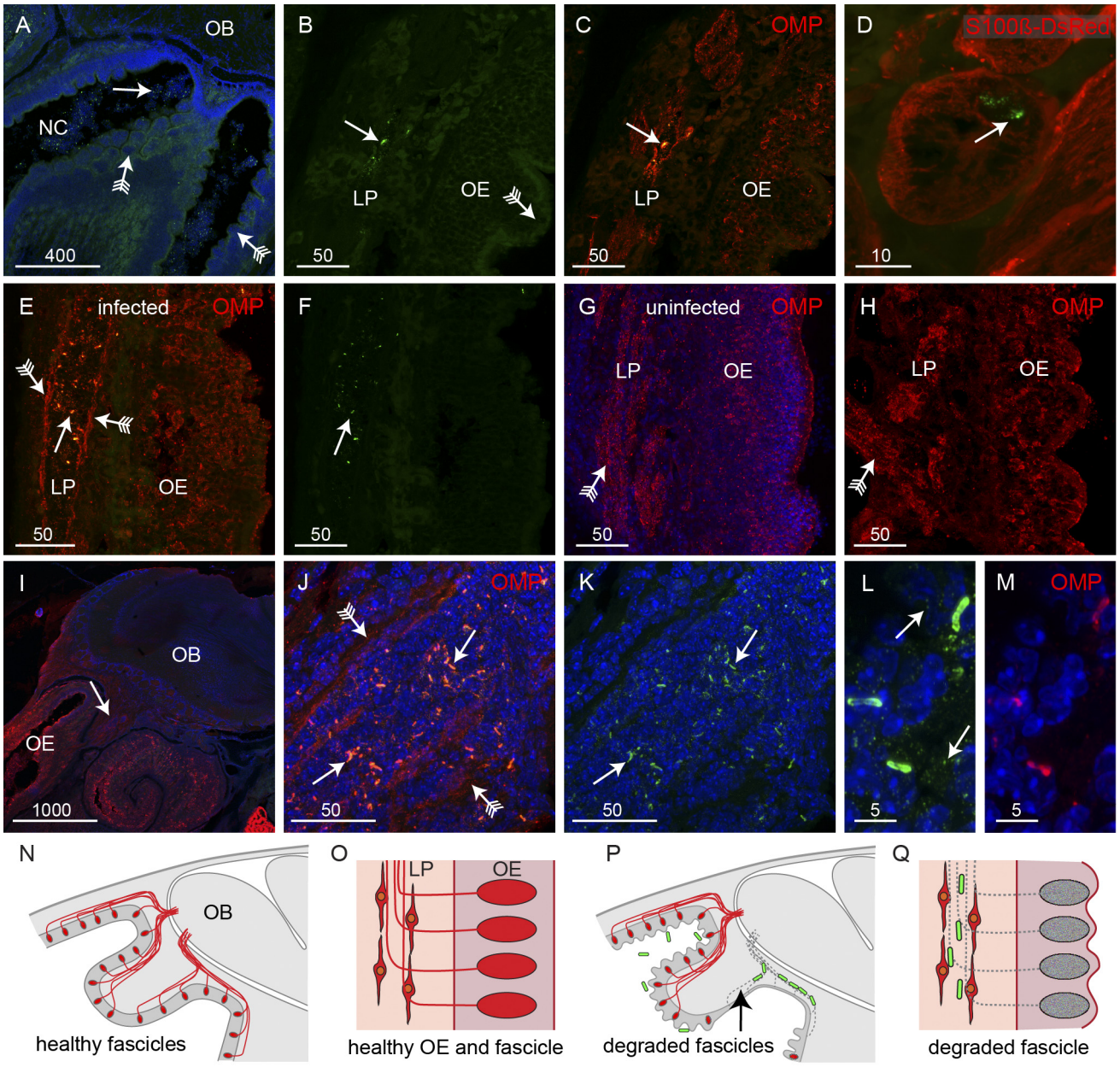

FIG 3 *B. pseudomallei* travels along olfactory nerve bundles. Sagittal sections were immunolabeled with anti-*B. pseudomallei* antibodies (green) and stained with DAPI (blue), with some sections also showing neurons (OMP antibodies; red) or glia (S100β-DsRed; red). (A) In regions of OE showing extensive crenellation (arrows with tails), bacteria (arrow) were present in the adjacent NC. (B and C) Double-label fluorescence. (B) Anti-*B. pseudomallei* (green). (C) Anti-OMP (red) and anti-*B. pseudomallei* (green). There was no evidence of bacteria penetrating the crenellated OE (arrow with tail), although bacteria were occasionally observed in axon bundles within the LP. Immunolabeling with anti-OMP (red in panel C) showed that axons surrounding the bacteria within the bundles had degraded and left a partially open conduit. (D) A cross section through an olfactory nerve bundle; olfactory ensheathing cells (red) are morphologically intact despite the presence of *B. pseudomallei* (arrow) within the nerve bundle; three-dimensional animation is shown in Movie S1 in the supplemental material. (E and F) When bacteria (arrow) were present in nerve bundles within the lamina propria, the axons were degraded, with OMP immunolabeling (red) restricted to the periphery of the bundles (arrows with tails), leaving an open conduit. (G and H) Examples of intact nerve bundles (arrows with tails) that were not infected with bacteria even though the epithelium showed signs of crenellation. (I to K) In the large nerve projecting toward the nerve fiber layer of the olfactory bulb (OB), bacteria (arrows) were localized to regions where axons were absent and OMP immunolabeling was restricted to the periphery (arrows with tails); the arrow in panel I points to the region shown in panels J and K, which is a double-label image, with panel K showing the image without OMP immunolabeling. (L and M) Immunolabeling with antibodies against *B. pseudomallei* (L) and OMP (M). (L) In addition to labeling the rod-like bacteria, the anti-*B. pseudomallei* antibodies also specifically labeled numerous vesicles in the vicinity of the bacteria. (N to Q) Schematics summarizing the infection of the axon fascicles. (N) Sagittal view of uninfected olfactory region with axons (red) projecting from the epithelium toward the OB. (O) Close-up of the healthy olfactory epithelium (OE) and lamina propria (LP) with OECs surrounding the axons in the LP. (P) In uninfected mice, some axons are degraded (arrow) and bacteria (green) migrate along the empty nerve fascicles. (Q) Close-up view demonstrating how the bacteria migrate along the empty nerve fascicles within the confines of the surrounding OECs. Bar sizes are in μm.

localized (arrows, Fig. 3J and K) and the OMP immunolabeling was restricted to the periphery of the fascicles (arrows with tails, Fig. 3J). It should be noted that the intact bacteria within the olfactory epithelium and axon fascicles were immunoreactive for the OMP antibodies (Fig. 3L and M), whereas bacteria within the nasal cavity and not in contact with the olfactory neurons were not immunoreactive for OMP antibodies (Fig. 2M to P). The antibodies against *B. pseudomallei* also specifically labeled tiny vesicles that were in the immediate vicinity of the rod-like bacteria (arrows, Fig. 3L; vesicles can also be seen dispersed around the bacteria in Fig. 3K); immunolabeling in regions where bacteria were not present did not result in detection of any vesicles (data not shown). The small vesicles which were immunoreactive to the anti-*B. pseudomallei* antibodies (arrows, Fig. 3L) were not labeled by the anti-OMP antibodies (Fig. 3M). In summary, in healthy uninfected animals, the olfactory sensory neurons project axons in fascicles through the lamina propria toward the olfactory bulb (Fig. 3N) with the fascicles surrounded by OECs (Fig. 3O). When infection causes loss of neurons from the epithelium, the axons are also degraded, resulting in open conduits through which the bacteria can migrate (Fig. 3P) within the confines of the surrounding OECs (Fig. 3Q).

***Burkholderia pseudomallei* enters the nerve fiber layer of the olfactory bulb by migrating along fascicles that are devoid of axons.** We next determined whether or not *B. pseudomallei* could enter the olfactory bulb in the central nervous system through the olfactory nerves. We found that the bacteria penetrated the nerve fiber layer, which is the outer layer of the olfactory bulb within the cranial cavity. The peripheral olfactory nerve fascicles pass through the bony cribriform plate to form the nerve fiber layer which is within the cranial cavity (Fig. 4A). In uninfected animals, the area in which olfactory axon fascicles merge together and enter the nerve fiber layer of the olfactory bulb showed uniform structural integrity (Fig. 4B). In infected animals, bacteria were present within the large nerve fascicles that projected toward the nerve fiber layer (Fig. 4C to E). At the region spanning the cribriform plate, bacteria were clearly present on both sides: within the axon fascicles of the lamina propria (peripheral nervous system), within the fascicles as they crossed through the cribriform plate (arrows, Fig. 4G and H), and in the nerve bundles within the nerve fiber layer (central nervous system) (Fig. 4F to H). We next examined the distribution of axons in regions where *B. pseudomallei* was present within the nerve fiber layer in the olfactory bulb using immunolabeling for OMP. We found that the distributions of bacteria in the nerve fiber layer were the same using wild-type and Δ*cap* mutant strains of *B. pseudomallei*. In animals inoculated with wild-type *B. pseudomallei*, in all regions where bacteria were present, immunoreactivity for OMP was low and scattered, indicating that the primary olfactory axons had degenerated and were absent (Fig. 4I to L). In contrast, in regions where bacteria were not present, OMP immunoreactivity was strong and uniform (Fig. 4I and M). Within the olfactory bulb of animals at 24 to 48 h after inoculation, bacteria were detected only within the nerve fiber layer and were not usually detected in the glomerular layer or deeper layers of the olfactory bulb (Fig. 4I and J). In summary, in healthy uninfected animals, axons from the olfactory sensory neurons pass through the cribriform plate and enter the nerve fiber layer, which is the outer layer of the olfactory bulb (Fig. 4N and O). In infected animals where the axons are lost, the bacteria can migrate along the axon fascicles, pass through the cribriform plate, and enter the nerve fiber layer within the olfactory bulb (Fig. 4P and Q).

***Burkholderia pseudomallei* infects the trigeminal nerve of the nasal cavity and travels along axon conduits devoid of axons.** Neurological melioidosis often presents with involvement of brain stem (1); one possible route of transmission to the brain stem is via the trigeminal nerve that innervates the nasal cavity and projects to the brain stem. We therefore examined the trigeminal nerve for the presence of *B. pseudomallei*. We cut serial coronal sections through the nasal cavity and olfactory bulbs (Fig. 5A) of S100β-DsRed transgenic mice which had been inoculated with the Δ*cap* mutant strain of *B. pseudomallei*. This fluorescent reporter transgenic mouse strain was used as it allows for the easy identification of the trigeminal nerve, since the glia that surround the nerve express the fluorescent protein DsRed. One branch of the trigeminal nerve innervates the rostral region of the respiratory epithelium (Fig. 5B); in this region of the nasal cavity, there is no olfactory epithelium. In contrast to invasion of the olfactory epithelium, which required degradation of the olfactory epithelium, the bacteria easily traversed the thin respiratory epithelium. Bacteria were detected within the respiratory epithelium lining the dorsal and septal surfaces (Fig. 5C and D) and were present within the trigeminal nerve underlying the respiratory epithelium (Fig. 5E). In adjacent sections, immunolabeling for the axonal marker β-tubulin III showed that axons were absent from the areas of the nerve in which bacteria were present (arrow, Fig. 5F). In contrast, in uninfected trigeminal nerves, β-tubulin III immunolabeling (trigeminal neurons do not express OMP) showed that trigeminal axons were uniformly distributed throughout the nerve (Fig. 5G). We traced the trigeminal nerve as it projected caudally along the dorsal nasal cavity. In all locations, *B. pseudomallei* was detected within the trigeminal nerve (Fig. 5H and I). In the more caudal regions of the nasal cavity, the trigeminal nerve projected alongside the olfactory nerve bundles. Anti-β-tubulin III labeled both the olfactory and trigeminal nerves (Fig. 5J). To distinguish between olfactory and trigeminal axons, we used immunolabeling with anti-OMP to selectively label olfactory axons (arrows, Fig. 5K), whereas the trigeminal axons were not labeled (dashed oval, Fig. 5K).

The trigeminal nerve passes from the nasal cavity into the frontal cranial cavity and traverses from the medial to the lateral side of the rostral olfactory bulb (Fig. 5N to Q). We were easily able to distinguish trigeminal axons from olfactory axons, as only the olfactory axons express OMP (Fig. 5P); further, trigeminal axons exhibited lower levels of β-tubulin III immunolabeling than did olfactory axons (Fig. 5Q). *B. pseudomallei* was present in the trigeminal nerve (arrow, Fig. 5O), but in this series of experiments, bacteria were not detected within the olfactory bulb. In more caudal positions, a branch of the trigeminal nerve projected along the lateral wall of the cranial cavity and bacteria were detected within at least one axon bundle encased by Schwann cells (Fig. 5R to U). Overall, *B. pseudomallei* had successfully penetrated the respiratory epithelium in the rostral nasal cavity, migrated along at least one Schwann cell-encased trigeminal nerve bundle that was devoid of axons, and passed into the cranial cavity, covering a total distance of over 9,000 μm in 48 h.

DISCUSSION

We show here extensive immunohistological evidence for brain infection by *B. pseudomallei* from olfactory epithelium and respi-

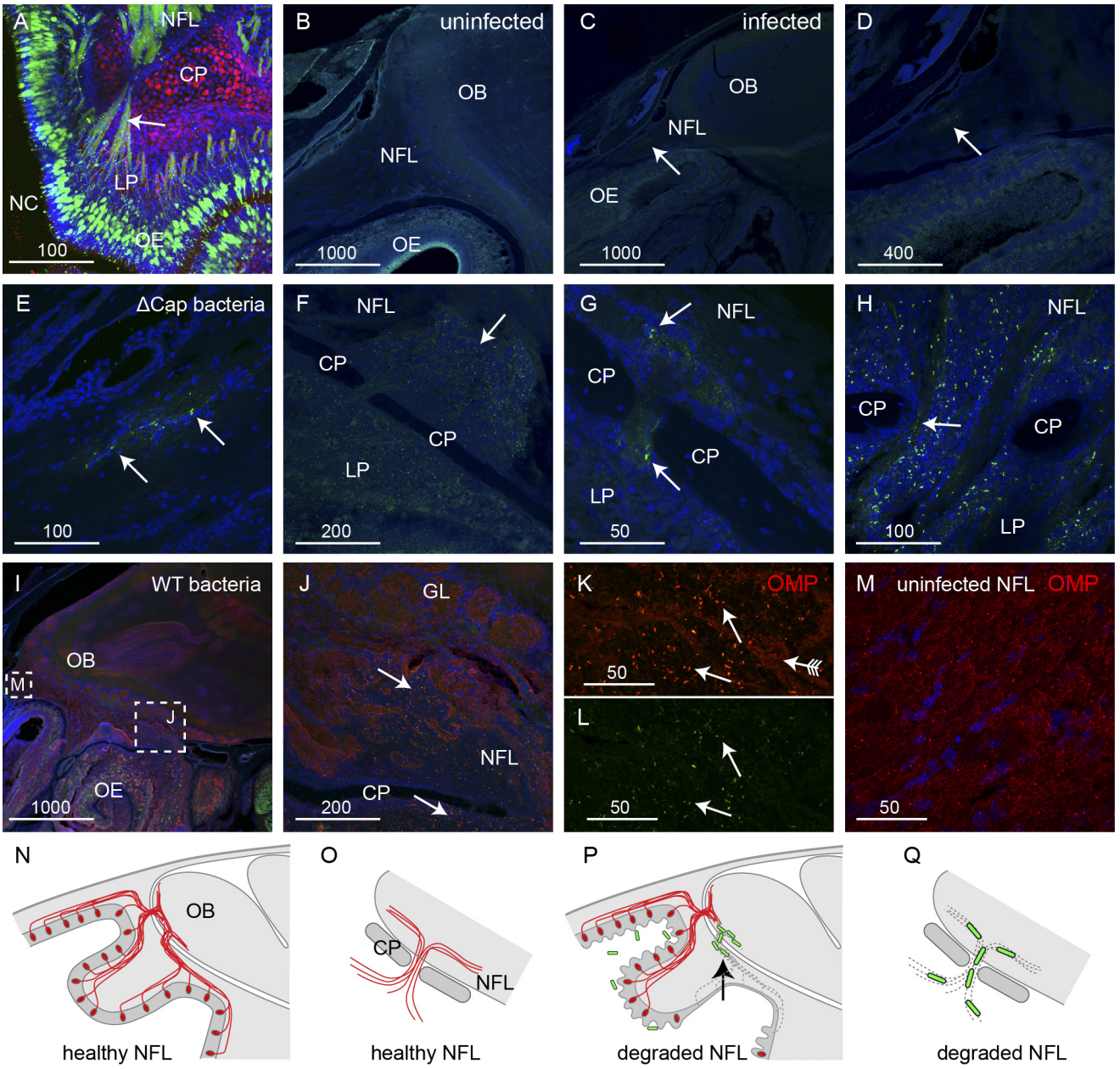

FIG 4 *B. pseudomallei* travels along the olfactory nerve to enter the olfactory bulb. (A) The olfactory nerve bundles (green; arrow) offer a direct route from the nasal olfactory epithelium (OE) to the nerve fiber layer (NFL) of the olfactory bulb. Panel A shows a sagittal section of an uninfected OMP-ZsGreen and S100β-DsRed transgenic mouse in which neurons are green and glia and chondrocytes are red. Panel B shows a sagittal section of an uninfected animal, and panels C to H show sagittal sections of animals infected with the Δ*cap* strain; sections are labeled with anti-*B. pseudomallei* antibodies (green) and DAPI (blue). (B) Uninfected olfactory nerve and olfactory bulb (OB). (C to E) Localized infection of the olfactory nerve projecting to the OB; the arrow points to *B. pseudomallei* (green); higher-magnification views of panel C are shown in panels D and E. (F) *B. pseudomallei* (green) infection was present in the lamina propria (LP) and ventral NFL (arrow). CP, cribriform plate. (G and H) Bacteria were present in the nerve bundles (arrow) passing through the cribriform plate (CP). (I to L) In animals infected with the wild-type (WT) strain of *B. pseudomallei*, the presence of bacteria (green) colocalized with regions of low OMP immunoreactivity (red). (I) Low-power sagittal view of the olfactory bulb; boxed areas are shown in panels J and M. (J) Bacteria (arrows) were present in the nerve bundles ventral to the CP and in the NFL. (K and L) Higher-magnification view of regions of panel J; OMP immunolabeling (arrow with tail) was high in regions where bacteria were absent but was low in regions where bacteria (green; arrows) were present. Panel L shows the same section as that in panel K but without OMP immunolabeling. (M) Higher-magnification view of boxed area shown in panel I at the rostral region of the NFL where no bacteria were present; the OMP immunolabeling is uniform, unlike that shown in panels J and K. (N to Q) Schematics summarizing the infection of the nerve fiber layer. (N) Sagittal view of uninfected olfactory region with axons (red) projecting into the olfactory bulb (OB). (O) Close-up view of axons passing through the cribriform plate (CP) and entering the NFL. (P) When axons are lost, *B. pseudomallei* migrates into the outer layer of the OB. (Q) Close-up view demonstrating how the bacteria migrate along the empty fascicles into the NFL. Bar sizes are in μm.

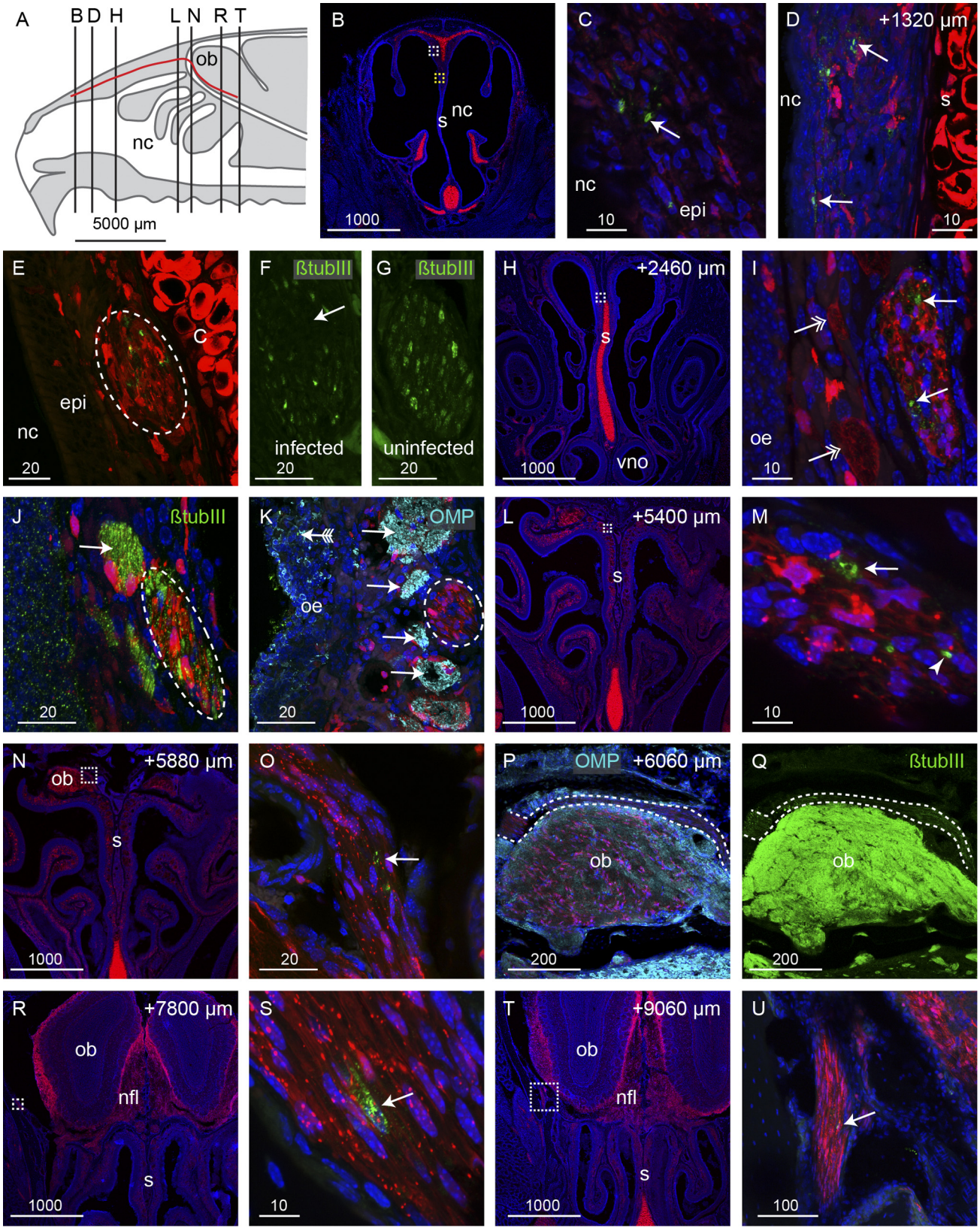

FIG 5 *B. pseudomallei* infection of the trigeminal nerve within the nasal cavity. (A) Schematic of the mouse nasal cavity (nc), olfactory bulb (ob), and branch of the trigeminal nerve (red line) with the locations of the following panels, which are coronal sections through an S100β-DsRed mouse head 48 h after inoculation; red fluorescence shows glia and chondrocytes; blue fluorescence is DAPI nuclear stain in all panels; dashed boxes show positions of higher-magnification views in the following sections. (B to D) Immunolabeling for *B. pseudomallei* (green; arrows in panels C and D) was localized to respiratory

(Continued)

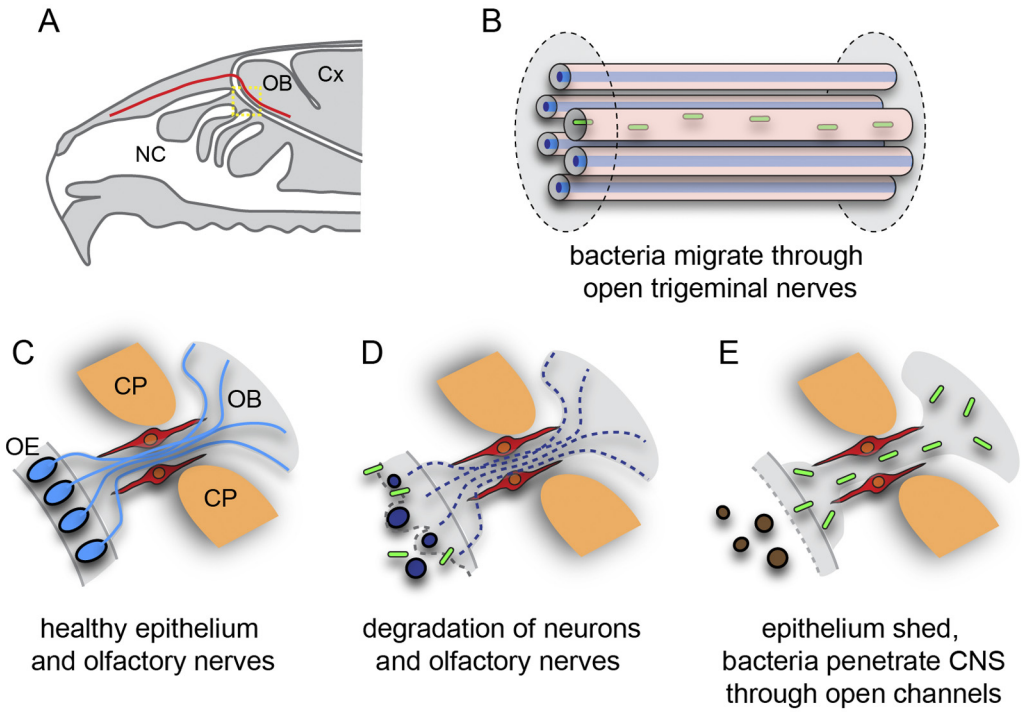

FIG 6 *B. pseudomallei* enters the central nervous system (CNS) via open channels. (A) Schematic sagittal view of the nasal cavity and olfactory system. The trigeminal nerve (red) is represented in panel B; the yellow boxed area is represented in panels C to E. (B) Some trigeminal nerve axons (blue) surrounded by Schwann cells degenerate as a result of the infection, and *B. pseudomallei* (green) migrates through the empty Schwann cell canals. (C) In healthy animals, primary olfactory neurons (blue) reside in the olfactory epithelium (OE) and project axons (blue lines) in nerve bundles through the cribriform plate (CP) into the olfactory bulb (OB) within the central nervous system. OECs (red) surround the nerve bundles. (D) Exposure to *B. pseudomallei* (green rods) results in neurons degrading (dark blue ovals) in some regions of the epithelium; the loss of the neuron cell bodies (brown ovals) from the epithelium leads to the degradation of their axons (dashed lines); OECs remain intact. (E) After the epithelium is sloughed off into the nasal cavity, the bacteria penetrate the remaining layers of the mucosa and migrate along the open channels left by the degraded axons and thereby enter the central nervous system.

ratory epithelia in the nasal cavity. The bacteria were able to migrate along olfactory and trigeminal nerve bundles and traverse the cribriform plate to enter the central nervous system within the cranial cavity within 24 h. We also show that bacterial colonization of the nasal lumen mucus by *B. pseudomallei* resulted in widespread crenellation of the olfactory epithelial surface followed by sloughing of the epithelial sheet, after which the bacteria were able to penetrate the remaining layers of the epithelium (Fig. 6).

The surface of the olfactory epithelium consists of homogeneously distributed supporting cells with dendrites of mature olfactory sensory neurons interspersed between, and protruding above, the supporting cells into the mucus layer of the nasal lumen (21, 22). We did not detect any evidence of bacteria selectively entering either the supporting cells or sensory dendrites. Nor was there evidence of the bacteria invading Bowman's glands, which secrete mucus through ducts and could offer a potential conduit from the nasal lumen through to the underlying lamina propria. Not even crenellation of the olfactory epithelium led to consistent colonization of the epithelium by the bacteria. Indeed, extensive bacterial invasion of the olfactory epithelium was detected only when the neuronal layer was sloughed off into the nasal cavity, exposing the underlying layers. These findings demonstrate that

Figure Legend Continued

epithelium (epi) on the dorsal portion of the septum (s; chondrocytes in the septum are red); the white box in panel B is enlarged in panel C; the yellow box in panel B shows the location of panel D in a section that is 1,320 μm more caudal; red fluorescence within the epithelium is localized within glia. (E) The trigeminal nerve that projects along the upper septum is infected; *B. pseudomallei* (green) appears within the trigeminal nerve (dashed oval). (F) A section adjacent to panel E shows β-tubulin III immunolabeling of the trigeminal axons (green); there is a noticeable loss of β-tubulin III in the area corresponding to where *B. pseudomallei* was localized in panel E. (G) In comparison, the trigeminal nerve in an uninfected animal shows uniform β-tubulin III immunolabeling across the nerve. (H to K) At a location 2,460 μm more caudal than that in panel B and in the location shown by the dotted box in panel H, bacteria (green; arrows in panel I) were present within the trigeminal nerve, which is distinguished by the tube-like Schwann cells; adjacent olfactory nerve bundles are indicated by double-headed arrows. (J and K) β-Tubulin III immunolabeling (green) (J) and olfactory marker protein (OMP) immunolabeling (cyan) (K) verified the identity of the trigeminal nerve (dashed ovals) in comparison to the adjacent olfactory nerve bundles (arrows). (K) The olfactory epithelium (oe) that was infected by bacteria (green; arrow with tail) was degenerated. (L to P) At locations 5,400 to 6,060 μm more caudal than that in panel B, the trigeminal nerve with degenerated particles of bacteria (arrows) or intact bacteria (arrowhead in panel M) entered the cranial cavity and passed over the rostral-dorsal region of the olfactory bulb. (P and Q) OMP (cyan) (P) and β-tubulin III (green) (Q) immunolabeling confirmed the identity of the trigeminal nerve in comparison to the olfactory axons that strongly express both OMP and β-tubulin III; dashed lines demarcate the trigeminal nerve. (R to U) The trigeminal nerve projected to the lateral portions of the cranial cavity, and immunolabeling for *B. pseudomallei* (green; arrows) was present in locations up to 9,060 μm caudal from panel B; boxed regions in panels R and T are shown at higher magnification in panels S and U, respectively. Bar sizes are in μm.

the olfactory nerve constitutes a direct conduit by which pathogens can rapidly invade the brain. This is consistent with a previous study which demonstrated that in healthy mice, the olfactory epithelium is an effective barrier against *Staphylococcus aureus* invasion; however, following damage to the olfactory epithelium by mild detergent treatment, *S. aureus* was detected in the olfactory epithelium and the olfactory bulb (23). Combined, these data suggest that significant damage to the olfactory epithelium may be a prerequisite for bacterial invasion of the olfactory nerves and olfactory bulb.

As olfactory axons project from the olfactory epithelium inward to the olfactory bulb, they group together to form nerve fascicles which are surrounded by olfactory ensheathing cells. When neuron cell bodies are lost, the axons rapidly die and are phagocytosed by the olfactory ensheathing cells (24), which maintain their positions and the overall integrity of the fascicles. Thus, the loss of axons from the fascicles results in open conduits extending from the nasal epithelium directly into the brain. We show clear evidence that the bacteria rapidly exploited this route and migrated along the open olfactory conduits that were devoid of axons so that within 24 h the bacteria had penetrated the outer layer of the olfactory bulb (Fig. 6C and D).

It is unknown whether *B. pseudomallei* virulence factors play a role in the cellular disruption and bacterial invasion of the olfactory epithelium and nerves. Recently, Cruz-Migoni et al. (25) described a *B. pseudomallei* toxin, structurally similar to *Escherichia coli* cytotoxic necrotizing factor 1, which demonstrated cytotoxic activity against J774.2 macrophages *in vitro*. However, an isogenic *B. pseudomallei* mutant deficient in this toxin still causes crenellation of the olfactory epithelium and destruction of olfactory neurons (data not shown). Alternatively, it is possible that crenellation and sloughing of the olfactory epithelium may occur as part of a host response against *B. pseudomallei* infection of the nasal cavity. Indeed, we have shown that *B. pseudomallei* induces a strong cytokine response in many tissues, including the olfactory epithelium (unpublished data). Further research to determine the role of *B. pseudomallei* virulence factors in the invasion of the olfactory pathway is warranted.

It is noteworthy that a feature of the bacterial infection was the presence of spherical particles which were selectively immunolabeled with the bacterial antisera. The size of these particles was approximately 200 nm, consistent with *B. pseudomallei* outer membrane vesicles (26). Outer membrane vesicles have a number of physiological functions, including the delivery of specific molecules to other cells through cell fusion (27). We speculate that the continual production of the vesicles may contribute to the destruction of the axons and hence facilitate the migration of the bacteria along the nerves. Thus, investigation of a possible role for *B. pseudomallei* outer membrane vesicles in infection is merited. Interestingly, the intact bacteria were reactive to the anti-OMP antibodies while the tiny vesicles were not. It has been previously reported that *Neisseria meningitidis* within the olfactory nerve colocalized with OMP immunolabeling (20). The reason for the bacterial immunoreactivity to OMP antibodies is unknown and worthy of further exploration.

The brain stem is a major site of signs and symptoms arising in neurological melioidosis, and the trigeminal nerve constitutes a direct pathway from the nasal cavity to the trigeminal nucleus in the brain stem (7). We clearly demonstrated that *B. pseudomallei* could easily penetrate the thin respiratory epithelium in the nasal cavity and colonize the trigeminal nerve. Bacteria were able to cross the intact respiratory epithelium, in contrast to the olfactory epithelium, which had to be damaged for bacteria to traverse it. Again, it was clear that the presence of the bacteria resulted in the loss of axons from within individual Schwann cell bundles, which likely facilitated the migration of bacteria along the trigeminal nerve into the cranial cavity. Thus, the trigeminal nerve bundles (Fig. 6B) from the nasal cavity provide a potential route to the brain stem in a manner essentially homologous to that of infection of the olfactory bulb. While we did not detect bacteria in the brain stem in this study, we could trace the bacteria a considerable distance along the trigeminal nerve within the cranial cavity, and it is possible that the bacteria could migrate even further and reach the brain stem or other brain areas if given more time.

In summary, we have provided evidence that *B. pseudomallei* penetrates the thin respiratory epithelium but penetrates the olfactory epithelium only once the neuronal layer has been sloughed off. The bacteria then migrate along nerves and pass through the cribriform plate to enter the cranial cavity. Thus, both the olfactory and trigeminal nerve routes offer a pathway into the brain by which the bacteria can bypass the blood-brain barrier.

MATERIALS AND METHODS

Bacterial strains and growth conditions. *B. pseudomallei* strain MSHR520 (previously "08" [28]) is a clinical isolate from a human case of melioidosis, donated by Bart Currie (Menzies School of Health Research, Darwin, Australia). An allele replacement capsule-deficient mutant of MSHR520 (MSHR520Δ*cap*) has been previously described (5). *B. pseudomallei* was grown in liquid Luria broth (LB) medium with shaking.

Mice and experimental infection. Unanesthetized female BALB/c mice (age, 5 to 10 weeks) and S100β-DsRed (29) mice were infected intranasally by placement of 10 μl of bacteria onto the nostrils (5 μl per nostril). The inoculum contained 3×10^5 stationary-phase cells resuspended in phosphate-buffered saline (PBS). Crosses of two transgenic reporter lines of mice, OMP-ZsGreen (30) and S100β-DsRed (29), were used to demonstrate the anatomy of the olfactory system. All protocols were approved by the animal ethics committee of Griffith University.

Immunohistochemistry and lectin chemistry. Animal tissue was prepared and cryostat sections were cut as previously described (31), and immunochemistry was performed as previously described (32). The primary antibodies used were rabbit anti-*B. pseudomallei* (1:2,000) (33), polyclonal goat anti-olfactory marker protein (OMP; 1:1,000; Wako), and polyclonal rabbit anti-β-tubulin III (1:500; Abcam) followed by the secondary antibody anti-rabbit Alexa Fluor 488 or anti-goat Alexa Fluor 594 (1:400; Invitrogen). The biotinylated lectin UEA1 (1:100; Dako) was incubated similarly to the antibodies, followed by streptavidin-Alexa Fluor 647 (1:400; Invitrogen). Cell nuclei were stained with 4′,6-diamidino-2-phenylindole (DAPI). Images were captured using an Olympus FV1000 microscope, and image panels were created using Adobe Illustrator CS3.

SUPPLEMENTAL MATERIAL

Supplemental material for this article may be found at http://mbio.asm.org/lookup/suppl/doi:10.1128/mBio.00025-14/-/DCSupplemental.

Movie S1, AVI file, 1.8 MB.

ACKNOWLEDGMENTS

This work was supported by a grant from the National Health and Medical Research Council, no. 1020394, to I.R.B., M.B., and G.U. and an Australian Research Council Fellowship to J.A.K.E., grant no. DP0986294.

REFERENCES

1. **Currie BJ, Ward L, Cheng AC.** 2010. The epidemiology and clinical spectrum of melioidosis: 540 cases from the 20 year Darwin prospective

study. PLoS Negl. Trop. Dis. **4:**e900. http://dx.doi.org/10.1371/journal.pntd.0000900.
2. **Cheng AC, Hanna JN, Norton R, Hills SL, Davis J, Krause VL, Dowse G, Inglis TJ, Currie BJ.** 2003. Melioidosis in northern Australia, 2001-02. Commun. Dis. Intell. Q. Rep. **27:**272–277.
3. **White NJ.** 2003. Melioidosis. Lancet **361:**1715–1722. http://dx.doi.org/10.1016/S0140-6736(03)13374-0.
4. **Currie BJ, Jacups SP.** 2003. Intensity of rainfall and severity of melioidosis, Australia. Emerg. Infect. Dis. **9:**1538–1542. http://dx.doi.org/10.3201/eid0912.020750.
5. **Owen SJ, Batzloff M, Chehrehasa F, Meedeniya A, Casart Y, Logue CA, Hirst RG, Peak IR, Mackay-Sim A, Beacham IR.** 2009. Nasal-associated lymphoid tissue and olfactory epithelium as portals of entry for *Burkholderia pseudomallei* in murine melioidosis. J. Infect. Dis. **199:**1761–1770. http://dx.doi.org/10.1086/599210.
6. **Currie BJ, Fisher DA, Howard DM, Burrow JN.** 2000. Neurological melioidosis. Acta Trop. **74:**145–151. http://dx.doi.org/10.1016/S0001-706X(99)00064-9.
7. **Koszyca B, Currie BJ, Blumbergs PC.** 2004. The neuropathology of melioidosis: two cases and a review of the literature. Clin. Neuropathol. **23:**195–203.
8. **Chadwick DR, Ang B, Sitoh YY, Lee CC.** 2002. Cerebral melioidosis in Singapore: a review of five cases. Trans. R. Soc. Trop. Med. Hyg. **96:**-72–76. http://dx.doi.org/10.1016/S0035-9203(02)90248-8.
9. **Aronsson F, Robertson B, Ljunggren HG, Kristensson K.** 2003. Invasion and persistence of the neuroadapted influenza virus A/WSN/33 in the mouse olfactory system. Viral Immunol. **16:**415–423. http://dx.doi.org/10.1089/088282403322396208.
10. **Barnett EM, Perlman S.** 1993. The olfactory nerve and not the trigeminal nerve is the major site of CNS entry for mouse hepatitis virus, strain JHM. Virology **194:**185–191. http://dx.doi.org/10.1006/viro.1993.1248.
11. **Kristensson K.** 2011. Microbes' roadmap to neurons. Nat. Rev. Neurosci. **12:**345–357. http://dx.doi.org/10.1038/nrn3029.
12. **Lundh B, Kristensson K, Norrby E.** 1987. Selective infections of olfactory and respiratory epithelium by vesicular stomatitis and Sendai viruses. Neuropathol. Appl. Neurobiol. **13:**111–122. http://dx.doi.org/10.1111/j.1365-2990.1987.tb00175.x.
13. **Mori I, Goshima F, Ito H, Koide N, Yoshida T, Yokochi T, Kimura Y, Nishiyama Y.** 2005. The vomeronasal chemosensory system as a route of neuroinvasion by herpes simplex virus. Virology **334:**51–58. http://dx.doi.org/10.1016/j.virol.2005.01.023.
14. **Plakhov IV, Arlund EE, Aoki C, Reiss CS.** 1995. The earliest events in vesicular stomatitis virus infection of the murine olfactory neuroepithelium and entry of the central nervous system. Virology **209:**257–262. http://dx.doi.org/10.1006/viro.1995.1252.
15. **Salinas S, Schiavo G, Kremer EJ.** 2010. A hitchhiker's guide to the nervous system: the complex journey of viruses and toxins. Nat. Rev. Microbiol. **8:**645–655. http://dx.doi.org/10.1038/nrmicro2395.
16. **Jarolim KL, McCosh JK, Howard MJ, John DT.** 2000. A light microscopy study of the migration of *Naegleria fowleri* from the nasal submucosa to the central nervous system during the early stage of primary amebic meningoencephalitis in mice. J. Parasitol. **86:**50–55. http://dx.doi.org/10.2307/3284907.
17. **Martinez J, Duma RJ, Nelson EC, Moretta FL.** 1973. Experimental *Naegleria* meningoencephalitis in mice. Penetration of the olfactory mucosal epithelium by *Naegleria* and pathologic changes produced: a light and electron microscope study. Lab. Invest. **29:**121–133.
18. **Dons L, Jin Y, Kristensson K, Rottenberg ME.** 2007. Axonal transport of *Listeria monocytogenes* and nerve-cell-induced bacterial killing. J. Neurosci. Res. **85:**2529–2537. http://dx.doi.org/10.1002/jnr.21256.
19. **van Ginkel FW, McGhee JR, Watt JM, Campos-Torres A, Parish LA, Briles DE.** 2003. Pneumococcal carriage results in ganglioside-mediated olfactory tissue infection. Proc. Natl. Acad. Sci. U. S. A. **100:**14363–14367. http://dx.doi.org/10.1073/pnas.2235844100.
20. **Sjölinder H, Jonsson AB.** 2010. Olfactory nerve—a novel invasion route of *Neisseria meningitidis* to reach the meninges. PLoS One **5:**e14034. http://dx.doi.org/10.1371/journal.pone.0014034.
21. **Danciger E, Mettling C, Vidal M, Morris R, Margolis F.** 1989. Olfactory marker protein gene: its structure and olfactory neuron-specific expression in transgenic mice. Proc. Natl. Acad. Sci. U. S. A. **86:**8565–8569. http://dx.doi.org/10.1073/pnas.86.21.8565.
22. **Hempstead JL, Morgan JI.** 1983. Monoclonal antibodies to the rat olfactory sustentacular cell. Brain Res. **288:**289–295. http://dx.doi.org/10.1016/0006-8993(83)90105-1.
23. **Herbert RP, Harris J, Chong KP, Chapman J, West AK, Chuah MI.** 2012. Cytokines and olfactory bulb microglia in response to bacterial challenge in the compromised primary olfactory pathway. J. Neuroinflammation **9:**109. http://dx.doi.org/10.1186/1742-2094-9-109.
24. **Su Z, Chen J, Qiu Y, Yuan Y, Zhu F, Zhu Y, Liu X, Pu Y, He C.** 2013. Olfactory ensheathing cells: the primary innate immunocytes in the olfactory pathway to engulf apoptotic olfactory nerve debris. Glia **61:**490–503. http://dx.doi.org/10.1002/glia.22450.
25. **Cruz-Migoni A, Hautbergue GM, Artymiuk PJ, Baker PJ, Bokori-Brown M, Chang CT, Dickman MJ, Essex-Lopresti A, Harding SV, Mahadi NM, Marshall LE, Mobbs GW, Mohamed R, Nathan S, Ngugi SA, Ong C, Ooi WF, Partridge LJ, Phillips HL, Raih MF, Ruzheinikov S, Sarkar-Tyson M, Sedelnikova SE, Smither SJ, Tan P, Titball RW, Wilson SA, Rice DW.** 2011. A *Burkholderia pseudomallei* toxin inhibits helicase activity of translation factor eIF4A. Science **334:**821–824. http://dx.doi.org/10.1126/science.1211915.
26. **Nieves W, Asakrah S, Qazi O, Brown KA, Kurtz J, Aucoin DP, McLachlan JB, Roy CJ, Morici LA.** 2011. A naturally derived outer-membrane vesicle vaccine protects against lethal pulmonary *Burkholderia pseudomallei* infection. Vaccine **29:**8381–8389. http://dx.doi.org/10.1016/j.vaccine.2011.08.058.
27. **Kulp A, Kuehn MJ.** 2010. Biological functions and biogenesis of secreted bacterial outer membrane vesicles. Annu. Rev. Microbiol. **64:**163–184. http://dx.doi.org/10.1146/annurev.micro.091208.073413.
28. **Brown NF, Beacham IR.** 2000. Cloning and analysis of genomic differences unique to *Burkholderia pseudomallei* by comparison with *B. thailandensis*. J. Med. Microbiol. **49:**993–1001.
29. **Windus LC, Claxton C, Allen CL, Key B, St. John JA.** 2007. Motile membrane protrusions regulate cell-cell adhesion and migration of olfactory ensheathing glia. Glia **55:**-1708–1719. http://dx.doi.org/10.1002/glia.20586.
30. **Ekberg JA, Amaya D, Chehrehasa F, Lineburg K, Claxton C, Windus LC, Key B, Mackay-Sim A, St. John JA.** 2011. OMP-ZsGreen fluorescent protein transgenic mice for visualisation of olfactory sensory neurons *in vivo* and *in vitro*. J. Neurosci. Methods **196:**88–98. http://dx.doi.org/10.1016/j.jneumeth.2011.01.008.
31. **Chehrehasa F, Windus LC, Ekberg JA, Scott SE, Amaya D, Mackay-Sim A, St. John JA.** 2010. Olfactory glia enhance neonatal axon regeneration. Mol. Cell. Neurosci. **45:**277–288. http://dx.doi.org/10.1016/j.mcn.2010.07.002.
32. **Chehrehasa F, Ekberg JA, Lineburg K, Amaya D, Mackay-Sim A, St. John JA.** 2012. Two phases of replacement replenish the olfactory ensheathing cell population after injury in postnatal mice. Glia **60:**322–332. http://dx.doi.org/10.1002/glia.22267.
33. **Boddey JA, Day CJ, Flegg CP, Ulrich RL, Stephens SR, Beacham IR, Morrison NA, Peak IR.** 2007. The bacterial gene lfpA influences the potent induction of calcitonin receptor and osteoclast-related genes in *Burkholderia pseudomallei*-induced TRAP-positive multinucleated giant cells. Cell. Microbiol. **9:**514–531. http://dx.doi.org/10.1111/j.1462-5822.2006.00807.x.